The presence of RNA cargo is suspected to modify the surface hydrophobicity of the MS2 phage

Guillaume Bastin, Christophe Gantzer, Evelyne Schvoerer, Guillaume Sautrey

▶ **To cite this version:**

Guillaume Bastin, Christophe Gantzer, Evelyne Schvoerer, Guillaume Sautrey. The presence of RNA cargo is suspected to modify the surface hydrophobicity of the MS2 phage. Virology, 2023, 585, pp.139-144. 10.1016/j.virol.2023.06.007 . hal-04727260

HAL Id: hal-04727260

https://hal.univ-lorraine.fr/hal-04727260v1

Submitted on 9 Oct 2024

HAL is a multi-disciplinary open access archive for the deposit and dissemination of scientific research documents, whether they are published or not. The documents may come from teaching and research institutions in France or abroad, or from public or private research centers.

L'archive ouverte pluridisciplinaire **HAL**, est destinée au dépôt et à la diffusion de documents scientifiques de niveau recherche, publiés ou non, émanant des établissements d'enseignement et de recherche français ou étrangers, des laboratoires publics ou privés.

Distributed under a Creative Commons Attribution - NonCommercial - NoDerivatives 4.0 International License

The presence of RNA cargo is suspected to modify the surface hydrophobicity of the MS2 phage

Authors and affiliation: Guillaume Bastin[1], Christophe Gantzer[1], Evelyne Schvoerer[1,2], and Guillaume Sautrey[1]

[1] Université de Lorraine, CNRS, LCPME, F-54000, Nancy, France

[2] Laboratoire de Virologie - Microbiologie, Hôpital Universitaire de Nancy, F-54500, Vandœuvre-lès-Nancy, France

Corresponding author: Dr. Guillaume Sautrey, tel: +33 3 72 74 74 12, email address: guillaume.sautrey@univ-lorraine.fr, ORCID: 0000-0002-8727-8931

Co-author email address: Dr. Guillaume Bastin: guillaume22.bastin@gmail.com, Pr. Christophe Gantzer: christophe.gantzer@univ-lorraine.fr, Pr. Evelyne Schvoerer: e.schvoerer@chru-nancy.fr

Abstract

The surface hydrophobicity of native or engineered non-enveloped viruses and virus-like particles (VLPs) is a key parameter regulating their fate in living and artificial aqueous systems. Its modulation is mainly depending on the structure and environment of the particles. Nevertheless, unexplained variations have been reported between structurally similar viruses and with pH. This indicates that some modulating factors of their hydrophobicity remain to be identified. Herein we investigate the potential involvement of RNA cargo in the MS2 phage used as non-enveloped RNA virus model, by examining the SDS-induced electrophoretic mobility shift (SEMS) determined for native MS2 virions and corresponding RNA-free VLPs at various pH. Interestingly, the SEMS of VLPs was larger and more variable from pH 5 to 9 compared to native virions. These observations are discussed in term of RNA-dependent changes in surface hydrophobicity, suggesting that RNA cargo may be a major modulator/regulator of this viral parameter.

Keywords

Surface hydrophobicity; non-enveloped virus; virus-like particle; protein-based nanocapsules; bionanoparticles; RNA cargo; coat protein; pH.

Introduction

Non-enveloped viruses, virus-like particles (VLPs), and other protein-based nanocapsules (PNCs) are promising candidates for the development of nanobiotechnologies. Examples include the use of native viruses that infect bacteria (*i.e.* bacteriophages; also known as phages) to combat multidrug-resistant strains (Kortright et al., 2019), virus-inspired platforms that display antigenic epitopes on their surface for vaccines (Lee et al., 2016), or nanocarriers designed as nucleic acid delivery vehicles for gene therapy (Giacca & Zacchigna, 2012). The success of applications is depending on the ability of particles to reach their target.

The ionic charge and hydrophobicity are the main physicochemical surface properties of viral particles and PNCs influencing their adsorption on biotic and abiotic substrates, which participates in the regulation of their fate in living or artificial aqueous systems. Therefore, fundamental knowledge about these surface properties and their variability must be acquired. Some advances have been provided concerning the surface hydrophobicity of considered particles thanks to model viruses like phages and developments of innovative techniques designed to estimate this parameter. It has been notably evaluated by monitoring the elution of virions in hydrophobic interaction chromatography (Heldt et al., 2017), their adsorption at the air/water interface (Hämmerling et al., 2017a, 2017b; Nguyen et al., 2011) and onto hydrophobic surfaces (Armanious et al., 2016; Dika et al., 2013; Hartard et al., 2021). It has also been explored by using the fluorescence properties of hydrophobic molecular probes (Brié et al., 2016; Heldt et al., 2017), from single-particle chemical force microscopy (Mi & Heldt, 2020) and surface tension measurements of water deposited onto surfaces adsorbed virions (Samandoulgou et al., 2021; Shi and Tarabara, 2018), or from *in silico* approaches (Armanious et al., 2016; Heldt et al., 2017; Meder et al., 2013). In this field,

we recently described a new method named “SDS-induced Electrophoretic Mobility Shift Assay” (SEMSA) (Bastin et al., 2022). The SEMSA consists of labelling the hydrophobic domains on the capsids with sodium dodecyl-sulfate (SDS) through non-polar interactions of the lipophilic tail of SDS molecules, exposing in their stead the negatively charged hydrophilic head (Sautrey et al., 2018). This increases the negative charge density of viral particles, altering their electrophoretic mobility measured by capillary zone electrophoresis (CZE). Such a shift can thus be interpreted in term of surface hydrophobicity, which is accurately quantified by subtracting the native from the SDS-modified electrophoretic mobility of particles, to define an “hydrophobic index” (*H*) increasing with their surface hydrophobicity. All data show that the surface hydrophobicity of viral particles is depending on the capsid surface exposure of hydrophobic amino acids, considering the 3D structure and organization of coat proteins. Concerning the effect of the viral environment such as pH, we showed by SEMSA that the *H*=f(pH) profile of several model viruses, namely the F-specific RNA phages MS2, Qβ and GA, is characterized by a phage-specific pH unit (called “pivotal pH”) where the *H* value changes suddenly (Bastin et al., 2022). We interpreted this effect as changes in surface hydrophobicity, supported by similar observations reported elsewhere (Hämmerling et al., 2017a). However, no studies have been specifically devoted to assessing the impact of other particle components besides coat proteins and some environmental parameters.

Herein, we focused our study on the RNA phage MS2 as a model to explore the potential impact of RNA cargo on the surface hydrophobicity of non-enveloped RNA viruses and RNA-loaded PNCs. We determined and compared the *H* values as a function of pH determined by SEMSA for native MS2 virions and analogous VLPs lacking the RNA component. The results show that the RNA cargo is a major modulator

and regulator of the *H*=f(pH) profile of MS2 phages, which can be interpreted as changes in surface hydrophobicity. This implies that potential relationships between surface hydrophobicity and RNA content of non-enveloped viruses, VLPs, and more generally RNA-loaded PNCs should be considered to predict their behavior in aqueous systems towards optimized applications.

Materials and methods

Chemical and reagents

Phosphoric acid solution ≥ 85%, phosphate salts, sodium chloride, dimethyl sulfoxide (DMSO), sodium dodecyl-sulfate (SDS) and other reagents in analytical grade were from Sigma Aldrich (Saint Louis, USA). Amicon® Ultra-0.5 centrifugal filter devices (100 kDa cutoff) were from Merck (Darmstadt, Germany). Ultrapure water was obtained in a Purelab Ultra MKII system from Elga (Le Plessis Robinson, France). All solutions were filtered through a 0.22 µm membrane (Alltech, Templeuve, France) prior to use. All experiments were performed at least in triplicate.

Production of MS2 phages and MS2 VLPs

The MS2 phages were produced, purified and enumerated as we previously described (Bastin et al., 2020). The typical concentration of purified phages in 1 mM PBS (13.7 mM NaCl, 0.27 mM KCl, 1.0 mM Na_2HPO_4, 0.18 mM KH_2PO_4, pH 7.4) was 5×10^{13} PFU/mL. The MS2 stock suspensions were stored at 4°C and away from light until use. They were used as starting material to prepare the MS2 VLPs by hydrolysis of the RNA cargo (Hooker et al., 2004), using Amicon® ultracentrifugal filter devices as described elsewhere for particle purification (Nguyen et al., 2011) with minor modifications in the protocol. Briefly, 10 µL of MS2 stock suspension were diluted in 440 µL of phosphate saline solution (100 mM Na_2HPO_4 + 100 mM NaCl) previously

buffered to pH 11.8 by adding the adequate volume of 1 M NaOH solution, washed twice with the same solution using 100 kDa Amicon® Ultra-0.5 centrifugal filter devices following the manufacturer's instructions, and incubated for 4h at room temperature away from light. The medium was then neutralized by two successive washes with low ionic strength phosphate solution (10 mM KH_2PO_4) previously buffered to pH 7.4 by adding the adequate volume of 0.1 M NaOH solution. The native MS2 phages were subjected to the same procedure but under neutral conditions for the first two washes and incubation (100 mM NaH_2PO_4 + 100 mM NaCl solution buffered to pH 7.4) where RNA hydrolysis is not promoted. The final volume of neutral- and alkaline-treated samples was ~20 µL, which corresponds to a ~2-fold dilution of the initial 10 µL of MS2 stock suspension. In order to normalize dilution and salt composition of all samples for all experiments, the neutral- and alkaline-treated samples were 2-fold diluted in 20 mM NaCl solution while the untreated MS2 stock suspension was 4-fold diluted in 13.3 mM NaCl solution.

Dynamic light scattering (DLS)

Normalized untreated MS2 stock, neutral- and alkaline-treated samples were diluted 10 times in 1 mM PBS. The average hydrodynamic diameter of particles in each sample was measured by dynamic light scattering (DLS) using a Zetasizer Nano ZS instrument (Malvern Instruments) as we previously described (Dika et al., 2013).

Capillary zone electrophoresis (CZE) and SDS-induced electrophoretic mobility shift assay (SEMSA)

CZE experiments were performed on a PA 800 *Plus* Pharmaceutical Analysis System apparatus equipped with a diode array UV detector operating between 200 and 300 nm for the acquisition of UV spectra of separate peaks (SCIEX) as we previously described (Bastin et al., 2022). The DMSO (neutral marker) then native or

VLP MS2 samples were successively injected at the inlet side of the capillary in the hydrodynamic forward mode, both sides of the capillary were immersed in the background electrolyte, and 10 kV voltage was applied (normal polarity). In this configuration, MS2 virions or VLPs migrate more slowly than DMSO, and the more their negative charge density, the longer is their migration time.

The hydrophobic index (*H*) of MS2 phages (H_{phage}) and analogous VLPs (H_{VLP}) were determined from CZE experiments for different pH as we previously described (Bastin et al., 2022). Briefly, samples (10 µL) were 2-fold diluted in 20 mM NaCl or 20 mM SDS solution (10 µL) prior injection in the CZE system, and analyzed by using a background electrolyte (10 mM ionic strength phosphate buffer at appropriate pH) supplemented with 10 mM NaCl or 10 mM SDS, respectively. The SDS-induced shift in the electrophoretic mobility of the particles for each pH was exploited to determine the H_{phage}=f(pH) and H_{VLP}=f(pH) profiles.

Statistical analysis of data

The statistical comparisons (*p*-value) used in text to evaluate the significance of the difference between two sets of *H* values were performed with GraphPad InStat v3.06 software from GraphPad Prism Software (San Diego, USA), using two-way ANOVA test followed by Bonferroni's posttest. The *p*-values <0.05 correspond to significant differences and the *p*-values <0.001 correspond to highly significant differences, while *p*-values >0.05 correspond to non-significant differences.

Results and discussion

The virions of MS2 phage consist of a genomic ssRNA cargo enclosed in a 28 nm capsid made from 178 copies of a single coat protein (CP) in three quasi-equivalent conformations A, B and C organized as 89 A/B or C/C dimers (Golmohammadi et al.,

160 1993). A unique copy of the A-protein (AP), involved in host recognition and infection,
161 is also incorporated (instead of hypothetical 90th dimer of CPs) to complete the capsid
162 arranged in a *T*=3 icosahedral lattice (Dent et al., 2013). Purified MS2 phages were
163 used as starting material to prepare MS2 VLPs by alkaline hydrolysis of the RNA cargo
164 (Hooker et al., 2004). The same procedure has been also successfully used to
165 generate VLPs derived from the nucleocapsid of hepatitis B virus (Strods et al., 2015).
166 The MS2 phages were parallelly subjected to the procedure under neutral conditions
167 to obtain native virions similarly as VLPs. First, analytical controls were performed to
168 ensure that MS2 VLPs were properly generated. As illustrated in Figure 1a, dynamic
169 light scattering (DLS) analyses confirmed that the nanoparticle structures were
170 preserved after neutral or alkaline treatment without aggregation (hydrodynamic
171 diameters of about 30 nm with satisfactory polydispersity of 0.12 ± 0.06 and 0.12 ±
172 0.01 for neutral- and alkaline-treated samples, respectively). However, the size
173 distribution of alkaline-treated samples (red) was slightly shifted towards larger
174 hydrodynamic diameters. This is consistent with previously published studies using
175 such treatments (Strods et al., 2015). Capillary zone electrophoresis (CZE) equipped
176 with a diode array UV detector (200-300 nm) was also employed for analytical purpose
177 (Kenndler and Blaas, 2001). Representative UV spectra of particles extracted from the
178 CZE analyses of MS2 stock suspension, neutral-treated and alkaline-treated samples
179 as well as the corresponding electropherograms are given in Figure 1b and 1c,
180 respectively. These data provide substantial information on the RNA content, recovery,
181 and surface ionic charge density of particles after treatment. The UV spectra obtained
182 for the neutral-treated samples (blue) were unchanged in comparison to the untreated
183 MS2 stock suspension (grey), both characterized by a maximum absorbance peak
184 located near 260 nm wavelength which is specific for RNA-containing samples

185 (Porterfield and Zlotnick, 2010). As expected, the maximum absorbance peak
186 observed for the alkaline-treated samples (red) was shifted to 280 nm wavelength,
187 which is characteristic for RNA-free MS2 particles (Hooker et al., 2004). Also, the
188 260/280 nm absorbance ratio determined for the neutral-treated samples (blue) was
189 1.88 while that of the alkaline-treated samples (red) was 0.78. These are typical values
190 for samples containing both RNA and proteins or samples containing only proteins
191 (Porterfield and Zlotnick, 2010; Sommer et al., 2003), which confirms the presence of
192 encapsulated RNA in neutral-treated samples or its removal in alkaline-treated
193 samples, respectively (Armanious et al., 2016; Wigginton et al., 2012). As illustrated in
194 Figure 1c, the migration peak for native MS2 phages (blue) appeared similar in terms
195 of peak intensity and position as the peak detected for untreated MS2 stock suspension
196 (grey), indicating a good recovery (87%, estimated from the maximum absorbance at
197 200 nm on the corresponding UV spectra given in Figure 1b) without change in the
198 surface ionic charge density of the particles after applying the ultrafiltration procedure.
199 The migration peak detected for the MS2 VLPs (Figure 1c red) was slightly enlarged
200 and shifted toward lower migration times compared to the one detected for native MS2
201 phages (Figure 1c blue), indicating a little heterogeneity and global decrease in the
202 anionic charge density of the particles after RNA clearance. This effect agrees with our
203 previous works showing the mild impact of the RNA cargo on the surface ionic charge
204 of MS2 virions (Langlet et al., 2008). The peak broadening leads to an apparent
205 decrease in peak intensity for MS2 VLPs (Figure 1c), but the maximum absorbance at
206 200 nm indicates a VLPs recovery of 78% from the starting MS2 stock suspension
207 (Figure 1b), also consistent with the literature (Hooker et al., 2004). Together, these
208 analytical controls confirm the preservation of chemical composition and structure for
209 native MS2 phages after neutral treatment, as well as slight structural changes

accompanying efficient degradation/removal of a large amount of the genomic RNA cargo after alkaline treatment.

To estimate and compare the apparent surface hydrophobicity as a function of pH between native MS2 phages and MS2 VLPs, the corresponding H_{phage} and H_{VLP} values were determined by SEMSA from pH 5 to 9. The SDS-induced shift in the electrophoretic mobility of particles for each pH, illustrated in Figure 2a for pH 9, was exploited to determine the H_{phage}=f(pH) and H_{VLP}=f(pH) profiles given in Figure 2b. It can be observed in Figure 2b that native MS2 phages (blue) displayed a very similar profile as we already published (Bastin et al., 2022), with relatively low and stable H_{phage} values from pH 9 to 7 (~0.13 ± 0.01, *p*-values >0.05 between each point) and a characteristic H_{phage}-jump from pH 7 to 5 reaching 0.55 ± 0.16 at pH 5 (*p*-value <0.05 between pH 7 and 6, *p*-value <0.001 between pH 6 and 5). Concerning MS2 VLPs (red), all the H_{VLP} values (*e.g.* 1.03 ± 0.06 at pH 8) were strongly higher than the H_{phage} values of native phages (0.13 ± 0.03 at pH 8, *p*-value <0.001), indicating that presence of the RNA genome decreases the SDS-induced shift in the electrophoretic mobility of MS2 virions. To give the reader with a relative scale, the *H* value at pH 8 we previously reported for the highly hydrophobic phage GA was 2.62 ± 0.31 (Bastin et al., 2022). The SEMSA results provided here for native MS2 virions and corresponding VLPs can thus be interpreted for modulation in surface hydrophobicity of particles. Such results and their interpretation are supported by the deviations in adsorption kinetics at the air/water interface and onto gold-chemisorbed dodecanthiol monolayers, i.e. at hydrophobic/hydrophilic interfaces, previously observed from native MS2 virions to MS2 VLPs prepared by alkaline treatment of the former (Armanious et al., 2016; Nguyen et al., 2011). It is currently accepted that the surface hydrophobicity of viral particles depends on the exposition and distribution of hydrophobic amino acids on the

outer surface of the proteinaceous capsid (Armanious et al., 2016; Heldt et al., 2017; Meder et al., 2013). This implies that the variations in hydrophobicity we measured by SEMSA after alkaline treatment should rely on some changes in these structural parameters affecting the SDS accessibility of hydrophobic domains on MS2 VLPs. In other words, alkaline treatment of native MS2 virions altered the hydration sphere of particles, as supported by slight variations in hydrodynamic diameter and electrophoretic mobility measurements here (Figure 1a and 1c), and elsewhere reported (Armanious et al., 2016; Nguyen et al., 2011; Strods et al., 2015; Wigginton et al., 2012). Assuming that most of the genomic RNA was cleared after alkaline treatment (or severely degraded), as shown here (Figure 1b) and in earlier studies (Armanious et al., 2016; Hooker et al., 2004; Nguyen et al., 2011; Wigginton et al., 2012), the question is: what component(s) of the viral shell is(are) specifically affected by RNA removal to modulate the capsid surface hydrophobicity, and by what mechanism(s)? The SEMSA procedure only provides information on the bulk hydrophobicity of particles surface without distinction between capsid components namely CPs and the AP for MS2 phage. However, although the AP is present in a single copy per capsid, it covers a large area of the outer surface impacting significantly the three-dimensional structure of the viral capsid (Dai et al., 2017; Koning et al., 2016; Kuzmanovic et al., 2006), and could thus influence the overall physicochemical surface properties of MS2 particles. Conservation of the AP in term of amount and structure after RNA release from native MS2 virions could be explored by protein and single particle analysis techniques, e.g. mass spectrometry (Bastin et al., 2020; Wigginton et al., 2012), or cryogenic electron microscopy (cryo-EM) (Luque and Castón, 2020), in order to assess its contribution to the effects observed in our hands. Recent progress in solving the atomic structure of whole MS2 virions and recombinant VLPs (lacking

the AP and genomic RNA cargo) can help us to strengthen the discussion. It has been notably shown that the RNA cargo inside wild-type MS2 virions adopts an asymmetric tertiary structure made from about sixty interconnected stem-loops, where the majority bind CPs and the AP from inside the capsid (Dai et al., 2017; Dent et al., 2013; Koning et al., 2016). Similar complex network between the genomic RNA and the capsid inner surface has also been observed in human viruses like hepatitis E virus (Xing et al., 2010). The capsid of MS2 phage (and probably that of other viruses) is thus asymmetric, the RNA-capsid binding regions being predominantly localized on one side containing the AP. In contrast, MS2 VLPs made from 180 copies of recombinant wild-type CP only and assembled in absence of the genomic RNA template are perfectly symmetric (de Martín Garrido et al., 2020). Interestingly, such VLPs exhibit symmetry variability between normal *T*=3 icosahedrons with an approximate diameter of 28 nm and *T*=4 variants (for which a fourth quasi-equivalent conformation of the CP has been observed) with a maximal diameter of ~33 nm. This is consistent with the hydrodynamic diameter measurements here shown in Figure 1a and those reported in another study (Strods et al., 2015). Hence, we propose that a transition may occur in native MS2 virions from the RNA-modeled asymmetric *T*=3 towards a mixture of symmetric *T*=3 and *T*=4 configurations upon removal of the genomic RNA template, leading to changes in the outer exposure of CPs and/or the AP that interacted with the removed RNA cargo. As we observed by SEMSA, the consequence would be a modulation in the SDS accessibility of hydrophobic domains localized on the affected region of capsids. This possible structural dynamics of MS2 particles after RNA removal will deserve further analysis by high resolution imaging like cryo-EM.

In addition to the comparison of hydrophobicity under specific conditions, the pH-dependent dynamics in *H* values displayed in Figure 2b for MS2 VLPs (red) and native

MS2 phages (blue) are significantly different. While the H_{VLP} and H_{phage} values decrease similarly from pH 5 to 6, the H_{VLP} value increases from pH 6 to 7 (from 1.05 ± 0.04 to 1.17 ± 0.05, *p*-value <0.05) whereas the H_{phage} value continues to decrease (from 0.28 ± 0.11 to 0.12 ± 0.02, *p*-value <0.05). Then the H_{VLP} value stays constant until pH 7.5, decreases between pH 7.5 and pH 8 (from 1.18 ± 0.05 to 1.03 ± 0.06, *p*-value <0.05) and keeps until pH 9, while the H_{phage} value stays constant from pH 7 to pH 9. The similar increase in H_{VLP} and H_{phage} values from neutral to acidic pH is easily attributable to approaching the isoelectric pH (~4) of MS2 particles (Dika et al., 2011), i.e. when the electrical surface charge of particles tends towards zero and they become more hydrophobic (Bastin et al., 2022; Dika et al., 2013, 2011). However, the variability in H_{VLP} values between neutral and alkaline pH cannot be explained in this way because the surface charge density of MS2 particles remains stable over the pH range 7-9 (Bastin et al., 2022; Dika et al., 2011). Based on the molecular flexibility of the MS2 capsid discussed above, the observation of several breaks in the H_{VLP}=f(pH) profile (i.e. from pH 6.5 to 7 and from pH 7.5 to 8) may rather be interpreted as pH-induced conformational rearrangements in CPs and/or the AP affecting the accessibility of external hydrophobic domains to the SDS probe. Such a structural dynamic has indeed been demonstrated in norovirus (structurally close to the MS2 phage) where, by twisting the flexible hinge connecting the CP dimers as pH increases (the precise mechanism is not yet clear), the protruding domain of CPs reversibly rotates with respect to the shell domain, which modify transiently the solvent accessibility of nearby secondary structures containing hydrophobic residues (Song et al., 2020). Interestingly, high variability in *H* values with significant *H*-jumps was only observed here for the MS2 VLPs, but not for native virions. These results support our proposal for greater capsid flexibility in absence of genomic RNA, affecting the hydrophobicity

variability of MS2 particles. Hence, we suggest that genomic RNA cargo in MS2 virions is involved in the modulation of this physicochemical parameter and its regulation in response to pH changes, by playing the role of a molecular anchor stabilizing the assembly and arrangement of CP dimers (Ni et al., 1995) and leading to a specific map of solvent accessibility over the capsid surface.

The previous hypotheses based on SEMSA results will need to be confirmed by complementary hydrophobicity measurement approaches and *in silico* estimations (Armanious et al., 2016; Heldt et al., 2017), as well as by structural characterizations using cryo-EM or Raman spectroscopy (Luque and Castón, 2020; Němeček and Thomas, 2009). Moreover, the specific role of CPs or the AP is missing which can be explored in future works by adding recombinant MS2 VLPs in the experimental setup. But they are still important for applications because they implie that the surface hydrophobicity of RNA-loaded viral particles cannot be deduced from the corresponding VLPs devoid of known RNA cargo, that it can vary unpredictably according to the solution's chemistry, and that it must thus be systematically characterized.

Conclusion

The data reported here show that presence of the RNA core in the MS2 phage affects strongly the SDS-induced shift in the electrophoretic mobility of particles. As discussed, these results can be interpreted as changes in apparent surface hydrophobicity according to the solvent accessibility of hydrophobic domains over the capsid surface, that is modulated by RNA-dependent arrangement of capsid proteins from the inside to the outside of particles. Moreover, this effect varies differently with pH between native MS2 virions and corresponding VLPs, supporting that RNA cargo

is also involved in the regulation of the pH-dependent variability of surface hydrophobicity of MS2 virions. Thus, this early work needs to be followed by further investigations to clarify the mechanism at the molecular level. Being of purely physicochemical origin, similar variability should also exist in other native or engineered non-enveloped RNA viruses, and more generally in RNA-loaded PNCs where the cargo interacts with coat proteins. Consequently, the hydrophobicity phenotype of such particles must be further investigated for a comprehensive understanding of their diffusion in aqueous systems toward optimized/new applications in medicine and for the environment.

CRediT authors contribution statement: Guillaume Bastin: Conceptualization, Formal analysis, Visualization, Writing – Original Draft, Visualization. **Evelyne Schvoerer:** Conceptualization, Writing – Review & Editing **Christophe Gantzer:** Writing – Review & Editing. **Guillaume Sautrey:** Conceptualization, Methodology, Validation, Formal analysis, Investigation, Resources, Writing – Original Draft, Writing – Review & Editing, Visualization, Supervision, Project administration.

Acknowledgement: We gratefully acknowledge Pr R. Duval, faculty director of Faculté de Pharmacie de Nancy (Université de Lorraine, Nancy, France), for access to the capillary electrophoresis instrument. We thank also J. Challant as well as Dr I. Bertrand, head of the technical platform Biologie Moléculaire Environnementale BME (UMR 7564 LCPME, CNRS-Université de Lorraine, Nancy, France), for assistance in phages production/purification and access to the BME platform, respectively. Additionally, we acknowledge the anonymous Reviewers for their valuable comments and suggestions to improve the paper. This work was supported by French Ministry of

Higher Education and Research and the French National Scientific Research Center (CNRS), as well as the University of Lorraine. This research received no external funding.

References

Armanious, A., Aeppli, M., Jacak, R., Refardt, D., Sigstam, T., Kohn, T., Sander, M., 2016. Viruses at Solid-Water Interfaces: A Systematic Assessment of Interactions Driving Adsorption. Environ Sci Technol 50, 732–743. https://doi.org/10.1021/acs.est.5b04644

Bastin, G., Gantzer, C., Sautrey, G., 2022. New method to quantify hydrophobicity of non-enveloped virions in aqueous media by capillary zone electrophoresis. Virology 568, 23–30. https://doi.org/10.1016/j.virol.2022.01.004

Bastin, G., Loison, P., Vernex-Loset, L., Dupire, F., Challant, J., Majou, D., Boudaud, N., Krier, G., Gantzer, C., 2020. Structural Organizations of Qβ and MS2 Phages Affect Capsid Protein Modifications by Oxidants Hypochlorous Acid and Peroxynitrite. Front Microbiol 11. https://doi.org/10.3389/fmicb.2020.01157

Brié, A., Bertrand, I., Meo, M., Boudaud, N., Gantzer, C., 2016. The Effect of Heat on the Physicochemical Properties of Bacteriophage MS2. Food Environ Virol 8, 251–261. https://doi.org/10.1007/s12560-016-9248-2

Dai, X., Li, Z., Lai, M., Shu, S., Du, Y., Zhou, Z.H., Sun, R., 2017. In situ structures of the genome and genome-delivery apparatus in a single-stranded RNA virus. Nature 541, 112–116. https://doi.org/10.1038/nature20589

de Martín Garrido, N., Crone, M.A., Ramlaul, K., Simpson, P.A., Freemont, P.S., Aylett, C.H.S., 2020. Bacteriophage MS2 displays unreported capsid variability assembling T = 4 and mixed capsids. Mol Microbiol 113, 143–152. https://doi.org/10.1111/mmi.14406

Dent, K.C., Thompson, R., Barker, A.M., Hiscox, J.A., Barr, J.N., Stockley, P.G., Ranson, N.A., 2013. The asymmetric structure of an icosahedral virus bound to its receptor suggests a mechanism for genome release. Structure 21, 1225–1234. https://doi.org/10.1016/j.str.2013.05.012

Dika, C., Duval, J.F.L., Ly-Chatain, H.M., Merlin, C., Gantzer, C., 2011. Impact of internal RNA on aggregation and electrokinetics of viruses: comparison between MS2 phage and corresponding virus-like particles. Appl Environ Microbiol 77, 4939–48. https://doi.org/10.1128/AEM.00407-11

Dika, C., Ly-Chatain, M.H., Francius, G., Duval, J.F.L., Gantzer, C., 2013. Non-DLVO adhesion of F-specific RNA bacteriophages to abiotic surfaces: Importance of surface roughness, hydrophobic and electrostatic interactions. Colloids Surf A Physicochem Eng Asp 435, 178–187. https://doi.org/10.1016/j.colsurfa.2013.02.045

Giacca, M., Zacchigna, S., 2012. Virus-mediated gene delivery for human gene therapy. Journal of Controlled Release 161, 377–388. https://doi.org/10.1016/j.jconrel.2012.04.008

Golmohammadi, R., Valegård, K., Fridborg, K., Liljas, L., 1993. The Refined Structure of Bacteriophage MS2 at 2.8 Å Resolution. J Mol Biol 234, 620–639. https://doi.org/10.1006/jmbi.1993.1616

Hämmerling, F., Lorenz-Cristea, O., Baumann, P., Hubbuch, J., 2017a. Strategy for assessment of the colloidal and biological stability of H1N1 influenza A viruses. Int J Pharm 517, 80–87. https://doi.org/10.1016/j.ijpharm.2016.11.058

Hämmerling, F., Pieler, M.M., Hennig, R., Serve, A., Rapp, E., Wolff, M.W., Reichl, U., Hubbuch, J., 2017b. Influence of the production system on the surface properties of influenza A virus particles. Eng Life Sci 17, 1071–1077. https://doi.org/10.1002/elsc.201700058

Hartard, C., Fenaux, H., Gentilhomme, A., Murray, J.M., Akand, E., Laugel, E., Berger, S., Maul, A., de Rougemont, A., Jeulin, H., Remen, T., Bensenane, M., Bronowicki, J.P., Gantzer, C., Bertrand, I., Schvoerer, E., 2021. Variability in molecular characteristics of Hepatitis E virus quasispecies could modify viral surface properties and transmission. J Viral Hepat 28, 1078–1090. https://doi.org/10.1111/jvh.13513

Heldt, C.L., Zahid, A., Vijayaragavan, K.S., Mi, X., 2017. Experimental and computational surface hydrophobicity analysis of a non-enveloped virus and proteins. Colloids Surf B Biointerfaces 153, 77–84. https://doi.org/10.1016/j.colsurfb.2017.02.011

Hooker, J.M., Kovacs, E.W., Francis, M.B., 2004. Interior Surface Modification of Bacteriophage MS2. J Am Chem Soc 126, 3718–3719. https://doi.org/10.1021/ja031790q

Kenndler, E., Blaas, D., 2001. Capillary electrophoresis of macromolecular biological assemblies : bacteria and viruses. Trends in Analytical Chemistry 20, 543–551. https://doi.org/10.1016/S0165-9936(01)00112-1

Koning, R.I., Gomez-Blanco, J., Akopjana, I., Vargas, J., Kazaks, A., Tars, K., Carazo, J.M., Koster, A.J., 2016. Asymmetric cryo-EM reconstruction of phage MS2 reveals genome structure in situ. Nat Commun 7, 12524. https://doi.org/10.1038/ncomms12524

Kortright, K.E., Chan, B.K., Koff, J.L., Turner, P.E., 2019. Phage Therapy: A Renewed Approach to Combat Antibiotic-Resistant Bacteria. Cell Host Microbe. https://doi.org/10.1016/j.chom.2019.01.014

Kuzmanovic, D.A., Elashvili, I., Wick, C., O'Connell, C., Krueger, S., 2006. The MS2 coat protein shell is likely assembled under tension: A novel role for the MS2 bacteriophage A protein as revealed by small-angle neutron scattering. J Mol Biol 355, 1095–1111. https://doi.org/10.1016/j.jmb.2005.11.040

Langlet, J., Gaboriaud, F., Gantzer, C., Duval, J.F.L., 2008. Impact of chemical and structural anisotropy on the electrophoretic mobility of spherical soft multilayer particles: the case of bacteriophage MS2. Biophys J 94, 3293–3312. https://doi.org/10.1529/biophysj.107.115477

Lee, K.L., Twyman, R.M., Fiering, S., Steinmetz, N.F., 2016. Virus-based nanoparticles as platform technologies for modern vaccines. Wiley Interdiscip Rev Nanomed Nanobiotechnol 8, 554–578. https://doi.org/10.1002/wnan.1383

Luque, D., Castón, J.R., 2020. Cryo-electron microscopy for the study of virus assembly. Nat Chem Biol. https://doi.org/10.1038/s41589-020-0477-1

Meder, F., Wehling, J., Fink, A., Piel, B., Li, K., Frank, K., Rosenauer, A., Treccani, L., Koeppen, S., Dotzauer, A., Rezwan, K., 2013. The role of surface functionalization of colloidal alumina particles on their controlled interactions with viruses. Biomaterials 34, 4203–4213. https://doi.org/10.1016/j.biomaterials.2013.02.059

Mi, X., Heldt, C.L., 2020. Single-particle chemical force microscopy to characterize virus surface chemistry. Biotechniques 69, 363–370. https://doi.org/10.2144/btn-2020-0085

Němeček, D., Thomas, G.J., 2009. Raman Spectroscopy in Virus Structure Analysis, digital Encyclopedia of Applied Physics. https://doi.org/10.1002/3527600434.eap670

Nguyen, T.H., Easter, N., Gutierrez, L., Huyett, L., Defnet, E., Mylon, S.E., Ferri, J.K., Viet, N.A., 2011. The RNA core weakly influences the interactions of the bacteriophage MS2 at key environmental interfaces. Soft Matter 7, 10449–10456. https://doi.org/10.1039/c1sm06092a

Ni, C.-Z., Syed, R., Kodandapani, R., Wickersham', J., Peabody, D.S., Ely, K.R., 1995. Crystal structure of the MS2 coat protein dimer: implications for RNA binding and virus assembly. Structure 3, 255–263. https://doi.org/10.1016/S0969-2126(01)00156-3

Porterfield, J.Z., Zlotnick, A., 2010. A simple and general method for determining the protein and nucleic acid content of viruses by UV absorbance. Virology 407, 281–288. https://doi.org/10.1016/j.virol.2010.08.015

Samandoulgou, I., Fliss, I., Jean, J., 2021. Adhesion of Norovirus to Surfaces: Contribution of Thermodynamic and Molecular Properties Using Virus-Like Particles. Food Environ Virol 13, 368–379. https://doi.org/10.1007/s12560-021-09471-3

Sautrey, G., Brié, A., Gantzer, C., Walcarius, A., 2018. MS2 and Qβ bacteriophages reveal the contribution of surface hydrophobicity on the mobility of non-enveloped icosahedral viruses in SDS-based capillary zone electrophoresis. Electrophoresis 39, 377–385. https://doi.org/10.1002/elps.201700352

Shi, H., Tarabara, V. v., 2018. Charge, size distribution and hydrophobicity of viruses: Effect of propagation and purification methods. J Virol Methods 256, 123–132. https://doi.org/10.1016/j.jviromet.2018.02.008

Sommer, J.M., Smith, P.H., Parthasarathy, S., Isaacs, J., Vijay, S., Kieran, J., Powell, S.K., McClelland, A., Wright, F., 2003. Quantification of adeno-associated virus particles and empty capsids by optical density measurement. Molecular Therapy 7, 122–128. https://doi.org/10.1016/S1525-0016(02)00019-9

Song, C., Takai-Todaka, R., Miki, M., Haga, K., Fujimoto, A., Ishiyama, R., Oikawa, K., Yokoyama, M., Miyazaki, N., Iwasaki, K., Murakami, K., Katayama, K., Murata, K., 2020. Dynamic rotation of the protruding domain enhances the infectivity of norovirus. PLoS Pathog 16, e1008619. https://doi.org/10.1371/journal.ppat.1008619

Strods, A., Ose, V., Bogans, J., Cielens, I., Kalnins, G., Radovica, I., Kazaks, A., Pumpens, P., Renhofa, R., 2015. Preparation by alkaline treatment and detailed characterisation of empty hepatitis B virus core particles for vaccine and gene therapy applications. Sci Rep 5, 11639. https://doi.org/10.1038/srep11639

Wigginton, K.R., Menin, L., Sigstam, T., Gannon, G., Cascella, M., Hamidane, H. Ben, Tsybin, Y.O., Waridel, P., Kohn, T., 2012. UV Radiation Induces Genome-Mediated, Site-Specific Cleavage in Viral Proteins. ChemBioChem 13, 837–845. https://doi.org/10.1002/cbic.201100601

Xing, L., Li, T.C., Mayazaki, N., Simon, M.N., Wall, J.S., Moore, M., Wang, C.Y., Takeda, N., Wakita, T., Miyamura, T., Cheng, R.H., 2010. Structure of hepatitis E virion-sized particle reveals an RNA-dependent viral assembly pathway. Journal of Biological Chemistry 285, 33175–33183. https://doi.org/10.1074/jbc.M110.106336

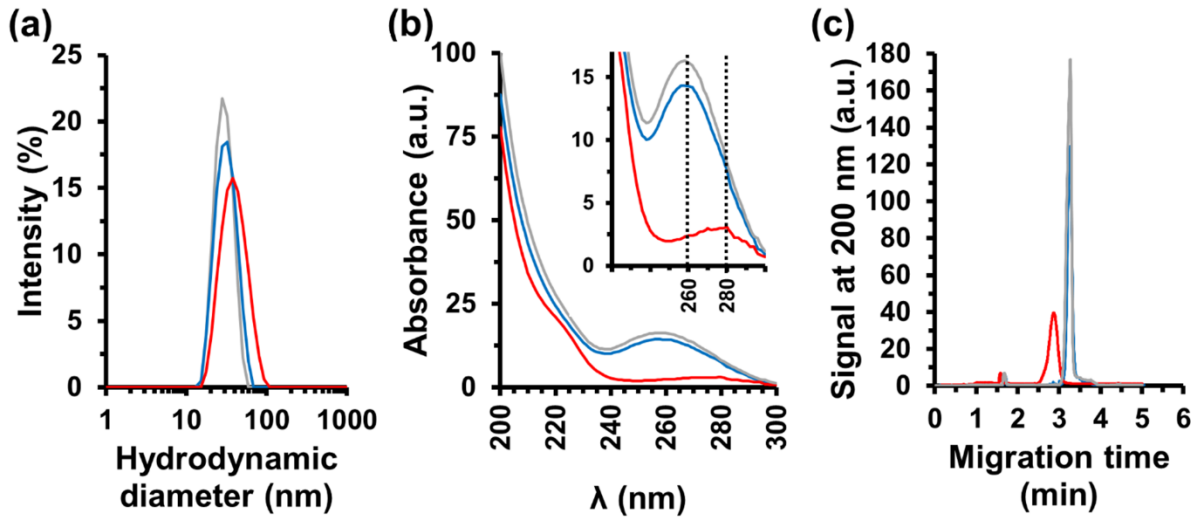

Figure 1. Dynamic light scattering (DLS) and Capillary zone electrophoresis (CZE)-UV analysis of native MS2 phages and VLPs. (a) Size distribution of particles in MS2 stock (grey), neutral-treated (blue) and alkaline-treated (red) samples. (b) Representative UV spectra of MS2 stock (grey), neutral-treated (blue) and alkaline-treated (red) samples, with enlargement near the 260-280 nm region. Data normalized according to the absorbance at 200 nm for MS2 stock samples (100%) (c) Representative electropherograms (detection wavelength 200 nm) obtained for MS2 stock (grey), neutral-treated (blue) and alkaline-treated (red) samples (background electrolyte pH 9 supplemented with 10 mM NaCl).

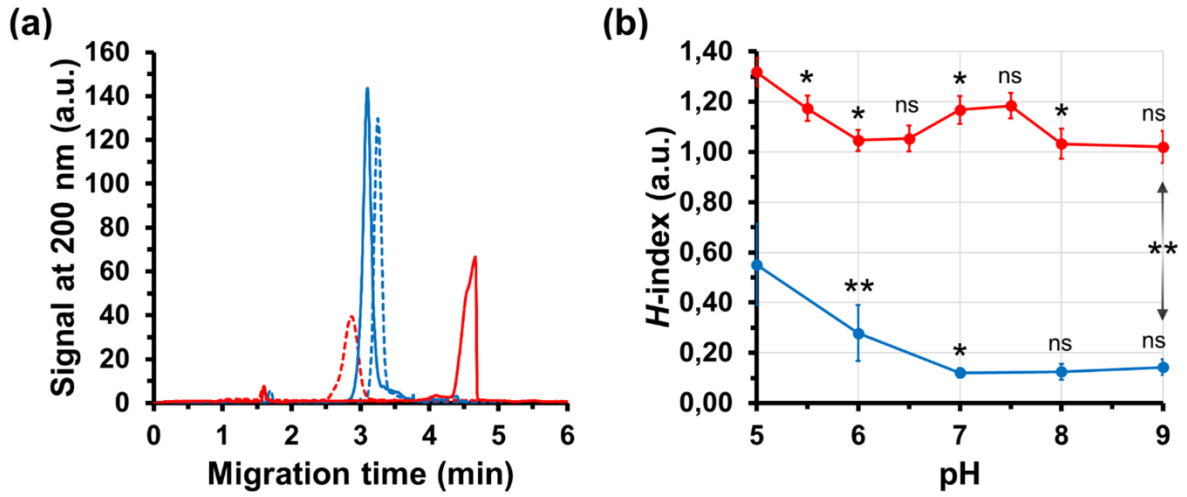

Figure 2. Apparent surface hydrophobicity of native MS2 phages and VLPs. (a) Representative electropherograms obtained by capillary zone electrophoresis (CZE) with SDS-free (dotted line) or SDS-containing (solid line) background electrolyte at pH 9 for native MS2 phages (blue) and VLPs (red). A shift of elution peaks to higher migration times indicates an increase in the negative charge density of SDS-labeled viral particles. (b) *H*=f(pH) profiles of native MS2 phages (blue) and VLPs (red). Error bars are SD. From pH 5 to pH 9, each set of values was statistically compared to the previous one: ns means not significant (*p*-values >0.05); * means significant (*p*-value <0.05); ** means highly significant (*p*-value <0.001). All experimental details related to the CZE analyses (a) and the *H* determination (b) are given elsewhere (Bastin et al., 2022).

506

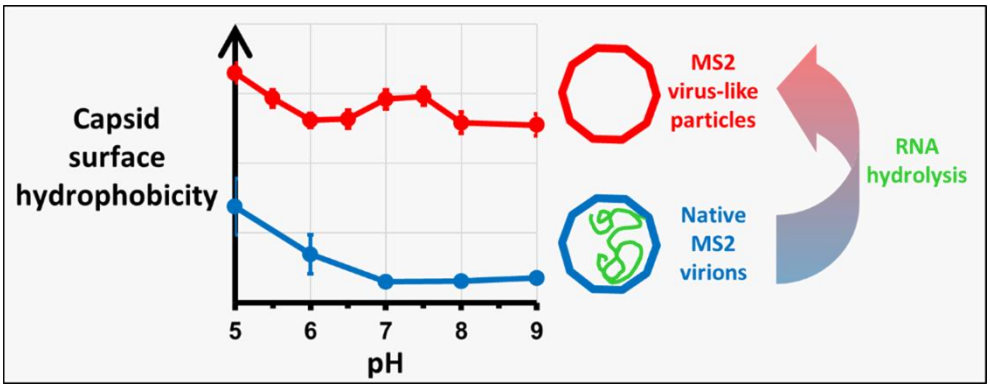
Capsid
surface
hydrophobicity
5
6
7
8
9
pH
MS2
virus-like
particles
Native
MS2
virions
RNA
hydrolysis